remote sensing

MDPI

Technical Note

Multitemporal and Multiscale Applications of Geomatic Techniques to Medium-Sized Archaeological Sites—Case Study of Marroquíes Bajos (Jaén, Spain)

Antonio Tomás Mozas-Calvache *, José Miguel Gómez-López and José Luis Pérez-García

Department of Cartographic, Geodetic and Photogrammetric Engineering, University of Jaén, 23071 Jaén, Spain
* Correspondence: antmozas@ujaen.es

Abstract: This study describes a methodology for obtaining a geometric documentation of a medium-sized archaeological area by applying various geomatic techniques. The procedure considers the obtainment of products at several scales, from the entire site to small artifacts, and at several dates, in order to model the evolution of the archaeological work. The methodology includes both LiDAR and photogrammetry, using the LiDAR point clouds to support the geometry obtained using photogrammetry and adding texture from this source. The technique used was adapted to the circumstances of the scene by considering the scale level (resolution and accuracy), complexity, and other requirements of the project. In the case of LiDAR, terrestrial laser scanning and structured-light scanning were used, and the aerial photogrammetry used two types of RPAS (medium and low flight height), close range photogrammetry with a conventional camera, and very close-range photogrammetry with a conventional camera mounted with a macro lens. The methodology demonstrated its feasibility for performing these types of studies, providing products adapted to the required scale level. All results were integrated into a website, including a map that allows user interaction and displays products at a selected zoom level, according to their scale level. The website also displays 3D models of the scenes and objects studied.

Keywords: TLS; photogrammetry; structured-light scanning; RPAS; 3D model

Citation: Mozas-Calvache, A.T.; Gómez-López, J.M.; Pérez-García, J.L. Multitemporal and Multiscale Applications of Geomatic Techniques to Medium-Sized Archaeological Sites—Case Study of Marroquíes Bajos (Jaén, Spain). *Remote Sens.* **2023**, *15*, 1416. https://doi.org/10.3390/rs15051416

Academic Editors: Giovanni Leucci, Nicola Masini, Salvatore Piro and Sebastiano D'Amico

Received: 20 January 2023
Revised: 28 February 2023
Accepted: 1 March 2023
Published: 2 March 2023

1. Introduction

The current possibilities for applying geomatic techniques to heritage, and specifically in archaeological sites, are enormous compared to those developed just a few decades ago. Those classical applications were mainly focused on obtaining cartographic documentation (e.g., contour maps), while more modern applications have opened up new possibilities, such as providing products (e.g., 3D models) for augmented reality, virtual museums, etc. The development of acquisition sensors, platforms, processing algorithms, and software and hardware capabilities, among other causes, are key to explaining the revolution experienced in this field in recent years. Thus, in these types of studies, we can highlight the large number of applications depending on photogrammetry and light detection and ranging (LiDAR), both terrestrial and aerial. In addition to the techniques applied to archaeological sites, we must also consider other data acquisition technologies, such as structured-light scanners, which are used to document small objects and artifacts. Therefore, one of the main factors to consider when using these techniques is the size of the scene or object to be studied, which will determine the scale. The scale, together with other requirements of the project, will have a great influence on the selection of the technique to be used, conditioning other aspects such as the resolution (GSD and point density) and data accuracy. In this context, Lambers and Remondino [1] categorized these techniques considering three scales: regional, local, and object. In the case of the medium-sized archaeological sites of several hectares, they considered local and object scales. Taking into account these scales, there is a wide range of geomatic techniques that can be applied, such as photogrammetry (aerial

and terrestrial, normal-case photogrammetry, and close range photogrammetry, etc.) and LiDAR (aerial and terrestrial, laser scanners, and structured-light scanners, etc.). Regarding multitemporal applications, most recent studies have focused on monitoring damages and restorations over a period of time [2] and the evolution of archaeological excavations [3,4], using both photogrammetric and LiDAR techniques. The selection of the technique to be implemented depends on various circumstances, such as the size of the site or scene (scale), the products to be obtained, the resolution and accuracy requirements, the availability of instruments, the complexity of the scene, the repeatability of the survey, etc.

The evolution of the photogrammetry applied to archaeological sites developed during the last decades can be summarized by considering several aspects, such as sensors, acquisition techniques, computing capabilities (hardware), and processing algorithms (software). The evolution of sensors is related to the expansion of the use of low-cost cameras, including pinhole cameras, 360-degree cameras, etc. [5–13]; and by mounting specific and special lenses, such as wide-angle lenses, macro lenses, and fisheye lenses [9,14,15], which facilitate data acquisition, due to the reduction of the number of photographs needed to cover the scene. In the context of acquisition techniques, the appearance of new platforms to lift cameras, such as remotely piloted aircraft systems (RPAS) [16–18], has allowed a revolution in the improvement in the efficiency of these photogrammetric surveys in contrast to other techniques, such as those based on masts [19–24] and balloons [6,25,26]. The use of RPAS allows us to survey archaeological sites (local scale), guaranteeing their execution with a defined flight height (scale consistency) and following a previous flight plan (ensuring defined overlaps). In this sense, classical aerial photogrammetry (considering the normal case with overlapping vertical photographs) has been improved by including other oblique images that ease orientation procedures and guarantee complete coverage by including images of possible vertical elements. An increase in the number of photographs used to cover a scene has been possible thanks to improvements in computing capabilities (hardware) and thanks to the development and implementation in software packages [27,28] of algorithms based on computer vision techniques, such as structure from motion (SfM) [29–32] and dense multi-view stereo (MVS) [32–35], which have eased the processing of photographs, allowing the use of photogrammetry by non-specialist users. This aspect implies the "democratization" of photogrammetry [36].

In the case of LiDAR, the great evolution of these techniques and their application to archaeological sites can be summarized considering aspects such as sensors, acquisition techniques, computer capabilities, and algorithm development (e.g., classification, registering, etc.). In the case of sensors, a classification according to the size of the scene can be made. Thus, there are aerial and terrestrial devices to cover distances at local scale (from 0.5 m to hundreds of meters), while other devices are specifically designed to cover a lower range of distances (less than 0.5 m) and are applied at object scale. In the case of aerial LiDAR, we highlight the recent use of sensors mounted on RPAS, which are mainly focused on surveying small and medium-sized areas [37,38], in contrast to those sensors mounted on board airplanes or helicopters, which are more focused towards large-sized areas [39,40]. Although the number of applications of aerial LiDAR in archaeology is increasing, if we consider studies of medium-sized sites, there has been a greater number of applications based on terrestrial laser scanning (TLS) [41–45], and this number is logically higher in applications of complex scenes and interior areas [46–48]. In this context, recent studies [49–51] have used portable mobile mapping systems (MMS) (e.g., Geoslam ZEB Go, Leica BLKGO, etc.) to survey complex spaces. MMS are composed of several sensors (acquisition sensors, navigation, and positioning sensors, and a time-referencing unit) that are synchronized to acquire data at high efficiency, achieving accuracies down to several centimeters [51]. Acquisition sensors are based on LiDAR and/or images, while navigation and positioning sensors are composed of global navigation satellite system (GNSS) receivers and/or inertial measurements unit (IMU) sensors. In cases where these sensors are not available, algorithms such as simultaneous localization and mapping (SLAM), have been developed to calculate the trajectory of the system based on point clouds or

images (LiDAR SLAM and Visual SLAM). MMS techniques represent a revolution in data acquisition, due to their high data capture efficiency.

The joint application of photogrammetry and TLS has demonstrated its feasibility in different studies, due to the improved acquisition efficiency and the advantages of the fusion of results. Several studies have demonstrated the benefits of this integration [41,43,44,52–55], taking advantage of their compatibility and the capabilities of each technique.

On the other hand, the evolution and use of techniques to document small objects and artifacts (object scale) have also been related to photogrammetry and LiDAR technologies. In the case of photogrammetry (e.g., very close range photogrammetry), the reduced size of the artifacts can cause some difficulties regarding the narrow field of view, minimum focusing distance, and focus range of the photographs, as well as the necessity for diffuse illumination. These problems are commonly solved by mounting macro lenses [56,57]; although, depending on the shape of the artifact, this requires the application of other acquisition strategies to complete the documentation (e.g., covering the object with a large number of photographs). Regarding LiDAR techniques, we highlight the use of short range laser scanners [58,59] and structured-light scanners [60–62] for obtaining 3D documentation of artifacts, either in situ or in the office.

Considering these premises, this study describes a methodology for developing the multitemporal and multiscale 3D documentation of an archaeological site. The main objective was related to obtaining accurate geomatic products considering several resolutions (scales) and related to four scene sizes (working subscales), and documenting the evolution of the archaeological work carried out on these scenes (pre- and post-archaeological excavation). In addition, we also included the integration of products in a common and open media (website) for dissemination, taking into account all dates and scenes documented.

This document is structured as follows: First, a description of the proposed methodology is given. Second, its application to a medium-size archaeological site containing remains from several epochs: Chalcolithic, Iberian-Roman, Visigoth, and Islamic periods is detailed. Finally, a description of the results obtained and the main conclusions of this study are presented.

2. Methodology

This study describes a new methodology for developing a geometric documentation of archaeological sites from the general to the particular and, consequently, from the lower scale level (complete zone) to the upper scale level (artifacts). Therefore, we define four scale levels (SL1 to SL4 in Figure 1), whose main characteristics are summarized in Table 1. First, the scale levels are defined by the area or dimensions of the scene, which largely governs the selection of the geomatic technique to be used. Second, we suggest values of GSD (case of using images) and point density (case of point clouds) related to each scale level SL1–SL4. These values are justified by a great number of studies described in the literature [1,3,4,17–22,24,26,48], although they will obviously depend on the requirements of each project, the available instruments, etc. The data acquisition related to the three levels SL1 to SL3 (site and test excavations) obviously took place in situ, while the object scale level acquisition took place in the office under controlled conditions (e.g., diffuse illumination).

Table 1. Summary of the scale levels considered in this study.

Scale Level	Description	Area/ Dimensions	GSD	Point Density
SL1	Full zone	>100 m^2	>10 mm	>5–10 cm
SL2	Test excavations covering tens of square meters.	10–100 m^2	1–10 mm	1–5 cm
SL3	Specific elements uncovered in test excavations of a few square meters.	<10 m^2	0.1–1 mm	<1 cm
SL4	Artifacts of a few centimeters	<10 cm	<0.1 mm	<0.1 mm

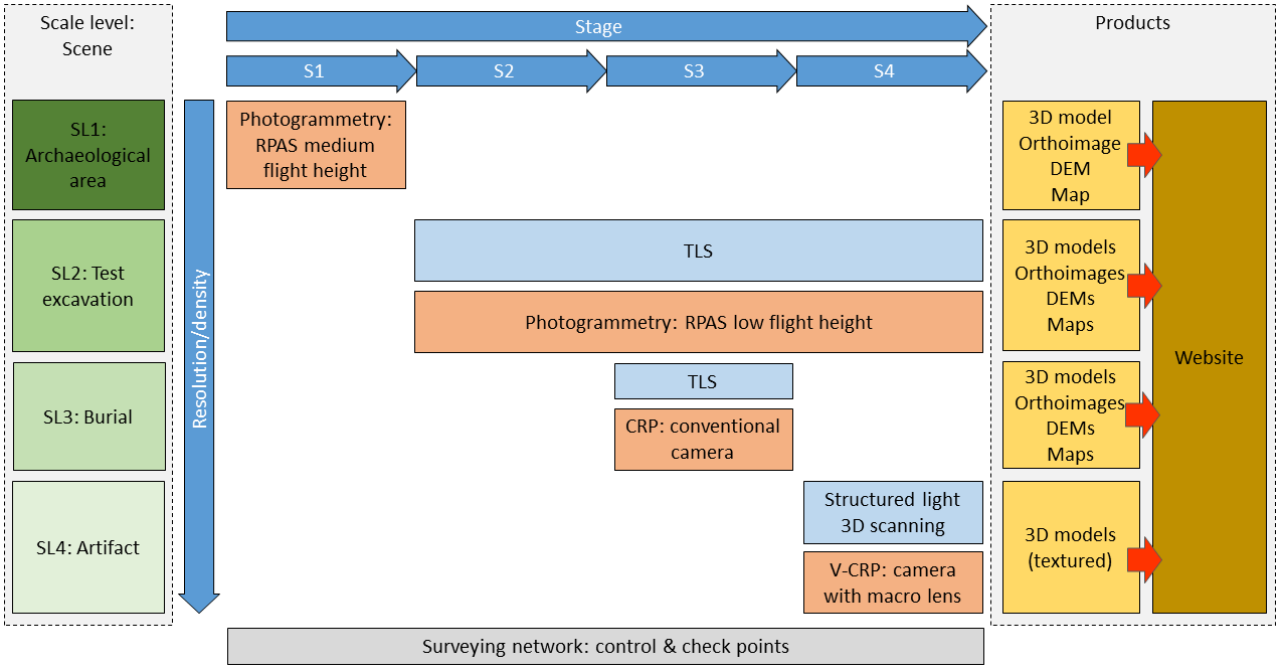

Figure 1. Methodology developed in this study.

In addition to the scale level, our approach also considers multi-temporal data acquisition, in order to document the evolution of the archaeological work. Considering the time variable, the methodology developed comprises four main stages (Figure 1):

- Stage 1 (S1): The purpose of this stage is the documentation of the initial state of the archaeological area (SL1) by obtaining cartographic products, in order to generate a base map to serve as a reference.
- Stage 2 (S2): This stage is related to the geometric documentation of the test excavations (SL2) prior to the archaeological intervention. The purpose is to document the initial status of these zones to be used as a reference for comparison with the situation during or after the excavations (e.g., volume of material removed).
- Stage 3 (S3): The third stage is focused on documentation of the test excavation (SL2) during the archaeological work and at an upper scale level (SL3) after the discovery of special elements found in the test excavation, such as burials. As described previously, these scenes cover several square meters. Therefore, this stage is implemented when the work developed in each test excavation is in progress.
- Stage 4 (S4): Finally, the fourth stage (T4 in Figure 1) is related to the documentation of the final situation of the excavation and includes two scale levels, the test excavation (SL2) (in situ) and the artifacts of interest (SL4) found during the archaeological intervention (in the office).

Taking into account these two variables, scale level and time, several geomatic techniques are considered, in order to document the scene geometrically during the evolution of the archaeological work (Figure 1). The selection of the geomatic technique should be based on the requirements of the project, the type and characteristics of the products to be obtained (e.g., considering the scale level; resolution or density), and the scene conditions (e.g., scene size). In this context, our approach considered the application of photogrammetry (both aerial and terrestrial), TLS, and structured light scanning. As a result, we considered obtaining various products to document the site, such as 3D models, orthoimages, digital elevation models (DEM), and maps. These products can be used to geometrically document the site before, during, and after the intervention. In addition to the geometric documentation, we proposed the implementation of a website (Figure 1)

considering all the results related to all scale levels and stages, in order to facilitate the dissemination of the project.

Obviously, all products must be referred to the same coordinate reference system (CRS). This implies the development of surveying tasks during all stages, including the definition of a surveying network distributed throughout the study zone and densified in the areas of interest of each stage. From this surveying network, several well-defined and well-distributed control points [63] and checkpoints (materialized using targets) are measured to georeference other products. Targets can be permanently installed, in order to reduce surveying tasks during the execution of the archaeological work, especially when these activities are distributed over several campaigns. Surveying tasks can be developed using GNSS devices and total stations, selecting in each case the most appropriate technique and methodology, and taking into account the scale level and the accuracy requirements of the project. In our approach, the coordinates of control points and checkpoints are mainly obtained from TLS point cloud (once georeferenced) (SL2–SL3), to reduce the surveying tasks. We recommend testing the accuracy of cartographic products following a standard, such as the one published by ASPRS [63], taking into account that the horizontal and vertical accuracy obtained must be consistent with the scale level.

As a general procedure, we propose the workflow shown in Figure 2, which describes the geomatic technique to be applied (surveying, TLS, and photogrammetry) and the products to be obtained for each scale level (SL1–SL4) (distributed by rows):

- SL1: First, we consider a general documentation of the site before the development of archaeological work, based on RPAS photogrammetry (Figure 2). In this case, we consider a medium flight height, to guarantee the acquisition of photographs and taking into account the GSD suggested in Table 1. A flight plan has to be defined considering all photogrammetric aspects (area, flight height, overlaps, focal length, GSD, etc.). We suggest the use of any software tool developed for this purpose, such as that described by Gómez-López et al. [64], to plan flights in complex scenarios. The processing includes the orientation of the photographs, and obtaining the point cloud and the texture. The results include various cartographic products to be used as a reference for the rest of the stages, such as the 3D models (including texture), orthoimages, DEMs, and maps.
- SL2: The scale level of test excavation is considered during several stages (S2–S4). In this case, we select TLS and photogrammetry using a RPAS to execute an aerial survey at a low flight height (Figure 2), to guarantee a complete coverture and the GSD requirement indicated in Table 1. The applications of TLS and photogrammetry are related, because the TLS products are complementary to the photogrammetric data, for obtaining complete documentation of the entire scene. The goal of TLS is to obtain the scene geometry and georeference the photogrammetric block, while the goal of photogrammetry is to obtain the geometry and texture for modelling. As a consequence, we suggest the use of TLS without RGB capture, in order to improve the acquisition efficiency. The location of the TLS stations must guarantee a complete coverage of the area, considering overlaps between adjacent point clouds, in order to ease the registering procedures. The point density should consider the requirements of the project and the need for high definition for the targets, in order to facilitate their identification in the point clouds. The TLS processing includes the registering of all point clouds to obtain a complete cloud and the XYZ transformation of this point cloud considering various points (targets). On the other hand, the photogrammetric process starts with the acquisition of photographs following a predetermined flight plan. Previous data (e.g., DEM) can be used to adjust the flight to the conditions and complexity of the scene [64]. The acquisition includes a complete set of normal-case vertical photographs and some oblique photographs, added to ensure complete scene coverage (e.g., to capture vertical elements). The orientation of the photographs and camera calibration are based on a set of well-distributed control points (targets), whose coordinates are extracted from the TLS point cloud (or occasionally from surveying)

and also checked using some additional points. After orientation of the photographs, a dense point cloud can be obtained by photogrammetry and can be compared to that obtained with TLS, to check for the presence of gaps. In this case, the photogrammetric point cloud is updated by adding the points from the TLS related to the missing zones. It should be noted that all points must contain information about the normal vector. Subsequently, the texture is obtained from the oriented photographs. As a result, we obtain 3D models (including texture), orthoimages, DEMs, and maps of the excavation test.

- SL3: This scale level includes the geometric documentation of some interesting elements found during the development of the archaeological field work (stage S3), such as burials. At this scale level, we select TLS and photogrammetry (Figure 2). As above, TLS is used to geometrically complement the data obtained from photogrammetry and to georeference the photogrammetric block. The scanning stations must be distributed around the element to be documented, and the acquisition must consider a higher density of points than in the previous case. The TLS processing is similar to the previous case. On the other hand, the photogrammetry is based on photographs obtained with a conventional camera mounted with normal lens and occasionally with macro lens, to capture details. The survey should be developed following the recommendations of the International Committee of Architectural Photogrammetry (CIPA) for architectural photogrammetric projects using non-metric cameras (known as 3×3 rules) [65,66]. These rules include photographic all-around coverage, which involves taking a ring of images around the object, with these images overlapping each other by more than 50% [65,66]. The orientation of photographs and camera calibration procedures are based on various control points, with coordinates obtained from the TLS. We also verify these processes using checkpoints obtained from both sources. As in the previous case, the photogrammetric point cloud is obtained by updating possible gaps using points extracted from the TLS. All points contain information about the normal vector. After that, the texture is calculated using the oriented photographs. The products obtained at this scale level are also 3D models, orthoimages, DEMs, and maps.
- SL4: The last scale level is developed in the office (stage S4) under controlled conditions using a structured-light scanner and very close-range photogrammetry (V-CRP) (Figure 2). Artifact scanning is developed using a turntable with coded targets, which facilitates the point alignment for obtaining a high density point cloud of the artifact. In the case of photogrammetry, we use a conventional camera mounted with a macro lens. The artifacts found during the archaeological field work are placed on a remotely controlled turntable that is inside a light box, providing diffuse illumination. We must develop several rings of images (blocks) [65,66] by moving the artifact after the acquisition of each block, in order to achieve full coverage of the object. The orientation of each block of photographs and camera calibration are developed using a set of targets with known coordinates located at the base of where the artifact is situated. The orientation between blocks is developed using common keypoints. After these procedures, we obtain a point cloud including information of normal vectors and a texture referenced in the same CRS. Both point clouds (scanning and photogrammetry) can be used individually or combined after referencing them in the same CRS. As in the previous cases, the texture is always obtained from the photogrammetry. The product obtained at this scale level is a 3D model of the artifacts with real texture.

The final step of the methodology described in this study includes the dissemination of all results in a single product that provides free online access. In this case, we select the development of a website (Figure 1), where most of the products will be available according to scale level and date. In this sense, we suggest the use of several web-mapping libraries to develop this website and that allow including orthoimages, DEMs, maps, and 3D models. The spatial coincidence of several products from the same area (obtained at several scale levels or stages) is solved by web-mapping using several layers, which can be shown or hidden by the users or considering the zoom level of the map view. In this sense, each

product (considering its scale level) is related to a range of zoom levels displayed in the map view. Table 2 shows the relationship proposed in this study between the scale levels (SL) and zoom levels applied in web-mapping based on ArcGIS API [67], Open Street Map [68], etc. In this sense, this approach suggests a range of zoom levels between 16 (visualization scale of about 1:9000) and 27 (visualization scale of about 1:4). This range of zoom levels is supported by several web-mapping libraries, such as OpenLayers, Leaflet, etc.

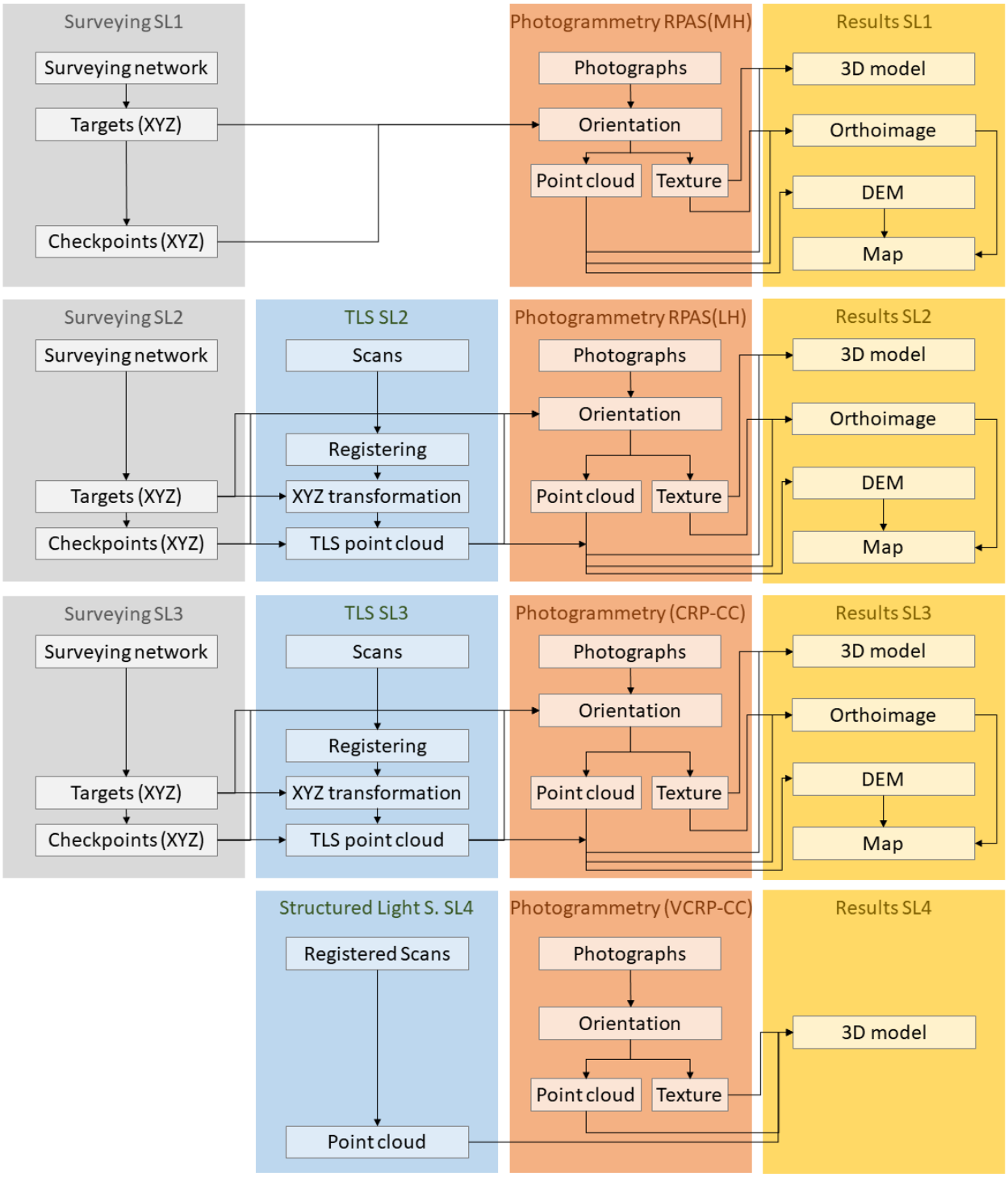

Figure 2. Workflow of the applications developed in this study, considering the scale level.

Table 2. Relationship between scale levels and web-mapping zoom levels.

Scale Level	Description	Minimum Zoom Level	Maximum Zoom Level
SL1	Full zone	16	22
SL2	Test excavations	20	27
SL3	Specific elements	22	27

3. Application

The methodology proposed in this study was applied to an area of about 6000 square meters included in the archaeological site of Marroquies Bajos. This site contains at least six concentric ditches from the chalcolithic period, distributed over a large area (about 100 hectares) and located within the urban area of Jaén (Spain) (Figure 3a). Due to the great extension of the site and considering its integration within the limits of an urban zone, the archaeological work has been developed for more than 30 years, dividing it into urban parcels, such as the one analyzed in this study. In this case, the zone to be studied (Figure 3b) is exclusively dedicated to the implementation of an archaeological park, due to its importance in the context of the site and its location (center of the Chalcolithic settlement), and the remains found in preliminary interventions (part of the first ditch is included in this zone). Therefore, the area to be studied contains multiple remains from the Chalcolithic to the Islamic periods. During the last few years, archaeological fieldwork has been carried out over several campaigns, in order to document this zone. In this context, a geometric documentation of the evolution of the archaeological interventions of each campaign was required. The archaeological work of each campaign focused on specific test excavations of about 100 square meters, which were completely excavated during that period. We had to consider the presence of some complex scenes remaining to be documented, such as a Roman well.

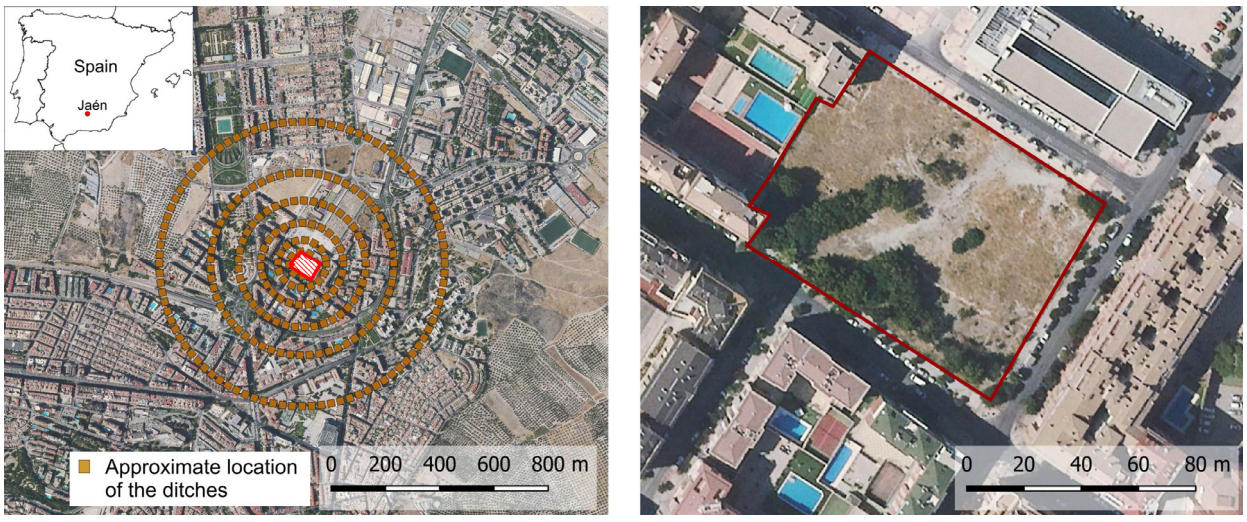

(**a**) (**b**)

Figure 3. Location of the archaeological area involved in this study: (**a**) location of Marroquíes Bajos; (**b**) archaeological area documented in this study.

The application of the methodology proposed in this study to the archaeological area of Marroquies Bajos was developed over several campaigns. Considering the scale level, the procedures carried out are summarized below:

- SL1: At this scale level, we developed a preliminary photogrammetric survey (S1) using an RPAS (DJI Phantom 4 RTK). In this application, we followed a predefined flight plan calculated to cover the whole scene with a medium flight height and thus obtain a GSD of about 1 cm. After acquisition, all photographs were processed using Agisoft Metashape software. The orientation procedure was initially based

on camera positions obtained from the GNSS-RTK sensor integrated into the RPAS, and subsequently this orientation was improved using several control points that were well-distributed throughout the area, as well as camera calibration, obtaining accuracies of about one centimeter based on the checkpoints. The coordinates of the control points and checkpoints were obtained from a GNSS RTK survey using a Topcon Hiper HR receiver. After orientation, we obtained a dense point cloud containing normal-vector information and a related texture. As a result, we obtained a 3D mesh, a 3D model (including texture), an orthoimage, a DEM, and a map of the archaeological area.

- SL2: This scale level included at least two stages of acquisition, before and after the archeological field work developed in each test excavation (S2 and S4), although in most cases (depending on the necessity for archaeological documentation) we also included surveys during the archaeological work (S3). The application related to SL2 included two geomatic techniques (Figure 4a): The TLS was based on a Faro Focus X130 scanner and the aerial photogrammetry was developed using an RPAS (DJI mini) to survey the scene at a low flight height (about 5 m). The use of this type of RPAS was justified considering the size at this scale level, the GSD demanded, the complexity of the scene, and the features of sensors usually mounted on these platforms. The point density selected for TLS acquisition (about 12 mm at 10 m) was related to the required final density (see Table 1) (considering overlaps between adjacent scans) and the need to capture targets with a certain level of detail, in order to obtain their coordinates properly. The TLS point cloud was obtained after the relative registering of all points clouds determined at all the scanning stations, which were well-distributed throughout the area, with the aim of covering it completely. After the relative registering of point clouds, a 3D transformation considering several targets (at least four) was developed, to obtain the final TLS point cloud that referred to the CRS of the project, obtaining accuracies of about 3 mm. The coordinates of the targets were obtained using a Leica TCRA1203 total station from the points of the local surveying network. These targets were permanently installed for use during the intervention (S2–S4), in order to reduce surveying tasks. On the other hand, the photogrammetric processing included the orientation of photographs and obtaining the point cloud and texture. These procedures were carried out using Agisoft Metashape software, obtaining accuracies of about 5 mm (based on a set of checkpoints). After the updating of the photogrammetric point cloud, we obtained several products (a complete 3D mesh, a 3D model (including texture), orthoimages, a DEM, and a map).
- SL3: This scale level included the geometric documentation of some interesting elements found during the development of the archaeological field work (stage S3), such as burials (Figure 4b). At this scale level (SL3), we used TLS and photogrammetry (Figure 4c,d). The TLS survey was based on a Faro Focus X130 scanner. The scanning stations were distributed around the element to be documented, obtaining high-density point clouds (density of 7 mm at 10 m). The registering was carried out relatively (cloud to cloud), obtaining a common point cloud. After that, we transformed this point cloud into the CRS of the project using a set of control points. On the other hand, the photogrammetry was based on photographs obtained with a conventional camera (Sony Alpha 6000) mounted with a normal lens (focal length of 30 mm) and occasionally with macro lens (focal length of 50 mm) to capture details. We included the acquisition of both normal-case and convergent photographs, covering the entire scene. In this sense, we used a mast to support the camera and a remote control to manage the framing and shooting of the camera. The orientation of photographs and camera calibration procedures were based on several control points with coordinates obtained from the TLS, and we verified these processes using other checkpoints. In this sense, the orientation procedure, carried out using Agisoft Metashape software, achieved accuracies of about 2 mm. Subsequently, a photogrammetric point cloud was

obtained by updating possible gaps using points extracted from the TLS. The products obtained during this stage were also 3D models, orthoimages, DEMs, and maps.

- SL4: The application of the last scale level was developed in the office (stage S4) using a structured-light scanner (3D Einscan Pro) (Figure 4e) and very close-range photogrammetry (V-CRP) using a conventional camera (Sony Alpha 6000) mounted with a macro lens (focal length of 50 mm) (Figure 4f). We obtained a high density point cloud of each artifact using both techniques, and the texture was obtained from photogrammetry. The results included a 3D model of each artifact.

Figure 4. Examples of applications developed in this study: (**a**) RPAS and TLS acquisition (SL2–S4) of an excavation test; (**b**) CRP acquisition of a burial (SL3–S3); (**c**) TLS acquisition of a Roman well (SL3–S4); (**d**) CRP acquisition of a Visigoth burial (SL3–S4); (**e**) structured-light scanning of an artifact (SL4–S4); (**f**) V-CRP acquisition of an artifact (SL4–S4).

The final step of the application included the development of a website for dissemination. Therefore, we developed a set of HTML documents hosted by a web server. These

web-pages included an element containing a map view that shows several layers related to the products obtained in this study. In this sense, we took advantage of some open-source web-mapping libraries. More specifically, we used the Leaflet library [69] based on JavaScript for the inclusion orthoimages and DEMs, and the 3DHOP framework, which is also based on JavaScript, for the creation of advanced web-based visual presentations of high-resolution 3D content [70,71]. The selection of both was related to the advantages of being open source libraries, their easy implementation thanks to the wide availability of examples and plugins (Leaflet), and the possibility of including high-resolution 3D models composed of a large amount of data (100 million triangles can be efficiently rendered in the case of 3DHOP). The Leaflet library allows displaying several georeferenced products, such as tiled images, sorted by layer. These layers represent levels of visualization, where a higher layer is displayed on top of a lower layer. In this context, we situated products of a higher scale level on top of products of a lower scale level. In any case, users can display or hide any product (layer) by selecting or unselecting items from an auxiliary menu. In the context of web mapping, the use of tiled images facilitates the management of georeferenced images at multiple resolutions because the tiles are pre-computed, which reduces the server workload and increases the interaction of users, due to the reduction of time between request and response. It is expected that the future archaeological park will contain panels with QR codes linking to this website.

4. Results and Discussion

The results obtained in this study are related to each application developed, considered the scale levels and the archaeological stages in which they were implemented. Figure 5 shows certain examples of these results. First, Figure 5a,b show some results of the complete archaeological area (SL1–S1), composed of an orthoimage of 2 cm (spatial resolution) and a topographic map, respectively. Figure 5c,d show two 3D models of two scenes related to excavation tests (SL2), containing part of the first chalcolithic ditch and a Roman well, respectively. The first case (Figure 5c) was surveyed just after starting the archaeological work (S2), while the second (Figure 5d) was obtained during the final stage (S4). We highlight the fact that despite of the great complexity of the Roman well, we obtained a complete 3D model of this area (video available in https://youtu.be/dlCCciZbi8Q, accessed on 16 February 2023). Two examples of the next scale level (SL3) and their implementation at stage S3 are shown in Figure 5e,f. Figure 5e shows a 3D model of a Visigoth burial (video available in https://youtu.be/Tnwn-8mmyAY, accessed on 16 February 2023). On the other hand, Figure 5f shows a 3D model of an Iberian burial (video available in https://youtu.be/KdCCwNK-AWU, accessed on 16 February 2023). Finally, Figure 5g,h show examples of 3D models obtained at scale level SL4 and stage S4. The first is related to a silex tool from the chalcolithic period of several centimeters, obtained using structured-light scanning (Figure 5g), while the second (Figure 5h) shows an example of a 3D model of a roman coin using V-CRP and two detailed views of it without texture and showing the wireframe. We highlight the great density of points obtained using both techniques at this scale level (see the wireframe meshes).

The methodology described in this study includes obtaining two point clouds of each scene by TLS and photogrammetry, at SL2 and SL3 scale levels. In these cases, the TLS point cloud is used to support the photogrammetric cloud in areas with gaps, but also to measure control and check points, to facilitate the orientation procedure. In this context, Figure 6 shows two examples of the results of the comparison of two TLS point clouds with the 3D models obtained using photogrammetry (Figure 6a,b). The distances between the TLS point clouds and the photogrammetric 3D models are categorized in intervals from zero to five centimeters, showing in most of cases values close to zero. These results are confirmed by the frequency plots of distance values shown in Figure 6c,d. In summary, the accuracy of the products obtained using these techniques was contrasted both using checkpoints (following ASPRS standard [63]) and by comparing their point clouds. As described in Section 3, the accuracy achieved was consistent with the products obtained

and the requirements of the project. In this sense, all products tested obtained values of RMSE consistent with the scale level of each product.

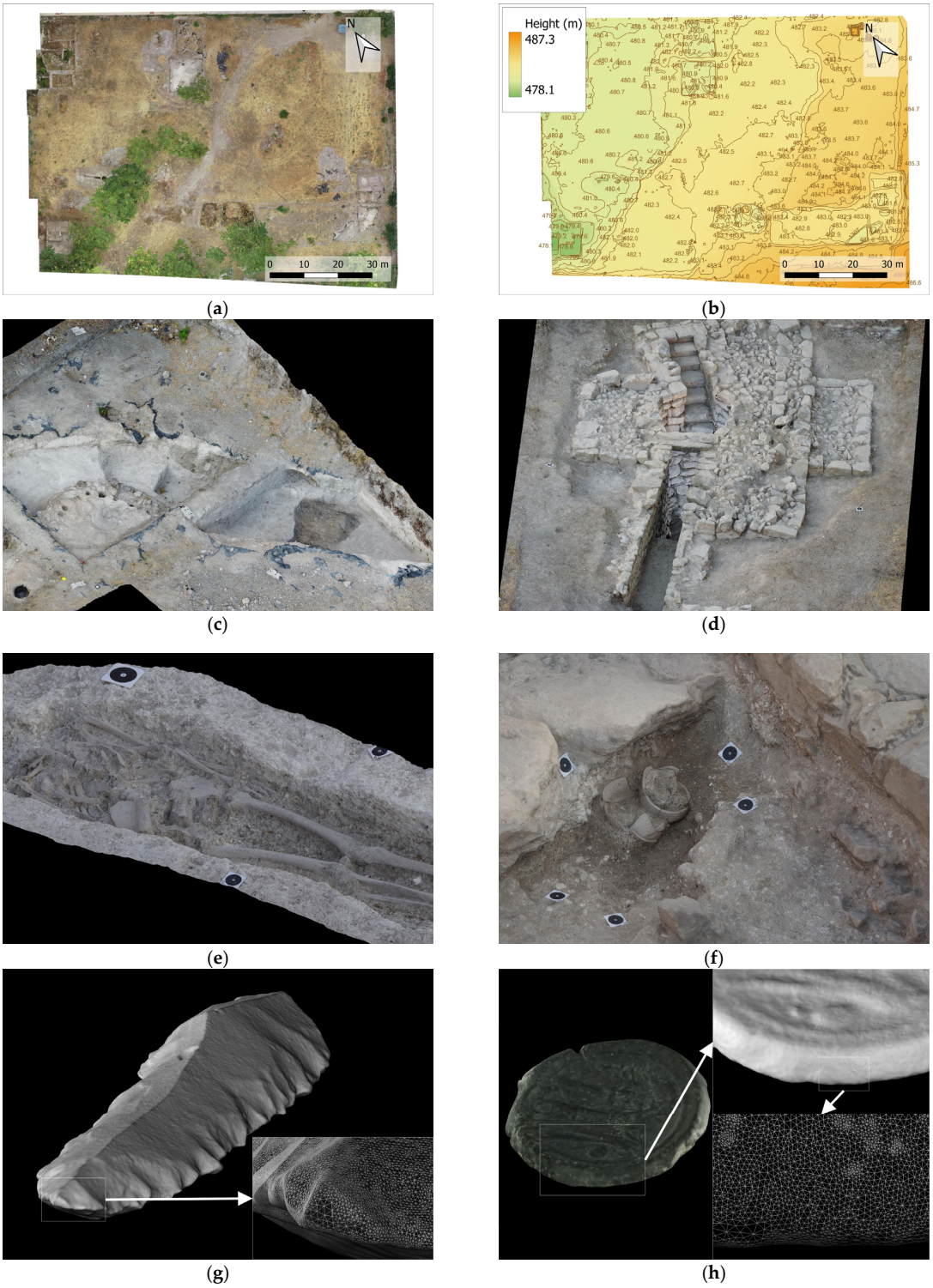

Figure 5. Examples of results obtained in this study: (**a**) orthoimage of the complete area (SL1–S1); (**b**) topographic map of the complete area (SL1–S1); (**c**) 3D model of the chalcolithic ditch (SL2–S2); (**d**) 3D model of a Roman well (SL2–S4); (**e**) 3D model of a Visigoth burial (SL3–S3); (**f**) 3D model of an Iberian burial (SL3–S3); (**g**) 3D model (structured-light scanning) of a silex tool and detail of the wireframe mesh (SL4–S4); (**h**) 3D model of a roman coin (SL4–S4) and detailed views without texture and showing the wireframe.

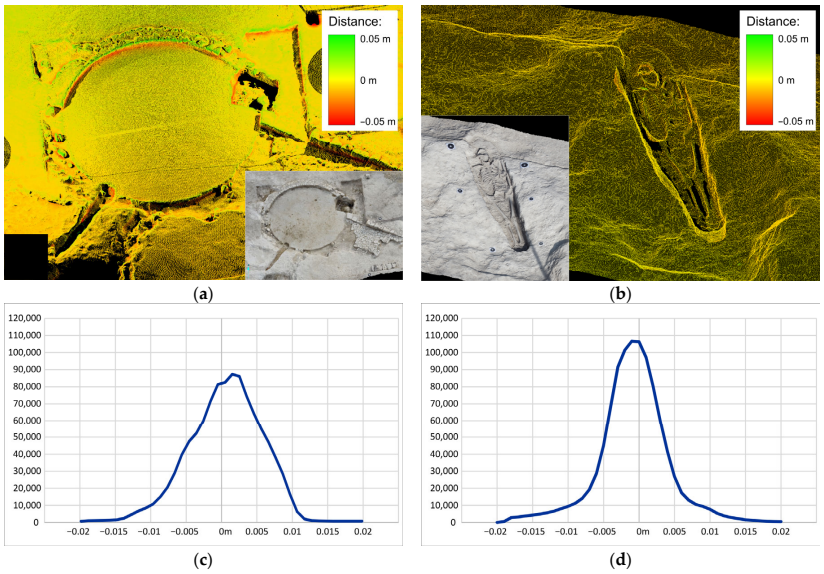

Figure 6. Comparison of TLS point clouds and 3D models obtained by photogrammetry: (**a**,**b**) distances from TLS points to 3D models; (**c**,**d**) frequency graphs of the cases (**a**,**b**).

One of the main goals of this study was the analysis of the evolution of the archaeological work carried out during test excavations. In this sense, Figure 7 shows several DEMs and 3D models regarding several stages of the archaeological work. Thus, Figure 7a shows a representation of four DEMs modelling the evolution of an archaeological test during the intervention. The documentation of each stage was decided following certain archaeological criteria. Figure 7b shows a 3D model obtained after the excavation process (S4) of an excavation test. The consequences on the modelling of the removal of material are displayed in Figure 7b, where the distances from this 3D model with respect to the initial situation are represented. In this case, the volume of excavation achieved was about 133.9 cubic meters. Considering another scale level (SL3), the comparison of the 3D model of one Visigoth burial once it was excavated (Figure 7c) with the initial state of this area shows a volume of excavation of about 2 cubic meters (Figure 7c). The volume estimation between 3D models was based on the distances calculated from a set of points extracted from a regular grid, previously obtained from one 3D model, with respect to the other 3D model. We used Maptek Point Studio software to calculate these distances. The volume was calculated considering the area of the zone and the average distance value. Another example of the evolution of the archaeological work is available in https://youtu.be/KdCCwNK-AWU, accessed on 16 February 2023.

The multi-temporal documentation carried out in this case study was developed at SL2 on several dates (at least before and after the archaeological work). The methodology proposed in this study allowed us to increase the number of documentations in each test excavation considering any archaeological criteria. For instance, following our approach, it was possible to develop a real-time acquisition, to obtain a progressive documentation of each archaeological layer by adding photogrammetric and TLS surveys at each stage of interest. The use of permanent targets is also aimed at reducing the surveying tasks in these multi-temporal works.

The website (https://coello.ujaen.es/proyectos/marroquies/, accessed on 16 February 2023) developed in this study (Figure 8) includes most of the products obtained (orthoimages and 3D models), including several scale levels and the stages of the archaeological work. The orthoimages are displayed on a map, using Google Maps as a background layer (Figure 8a), thanks to the referencing applied to all products of the project using a global CRS (EPSG:25830). Considering the zoom level of the map included in the webpage and selected by the user, several layers are shown or hidden. Thus, the selection of a general zoom level allows the visualization of the general orthoimage of the archaeological area (SL1–S1).

With the increase of the zoom level, the orthoimages of the test excavation (SL2–S4) are displayed (Figure 8b). After that, certain orthoimages of features are shown at a certain zoom level, such as burials (Figure 8c). These orthoimages are related to SL3–S3. All elements are included in an attached menu that allows users to show or hide them. These elements are sorted by scale level and date. Finally, each surveyed element or area (test excavation, burial, artifact, etc.) includes a link to display the related 3D model (Figure 8d). The 3D model is displayed in a new tab and allows users to interact with it. In this sense, users can navigate by rotating and panning the model, measure distances, apply sections, show/hide texture, etc.

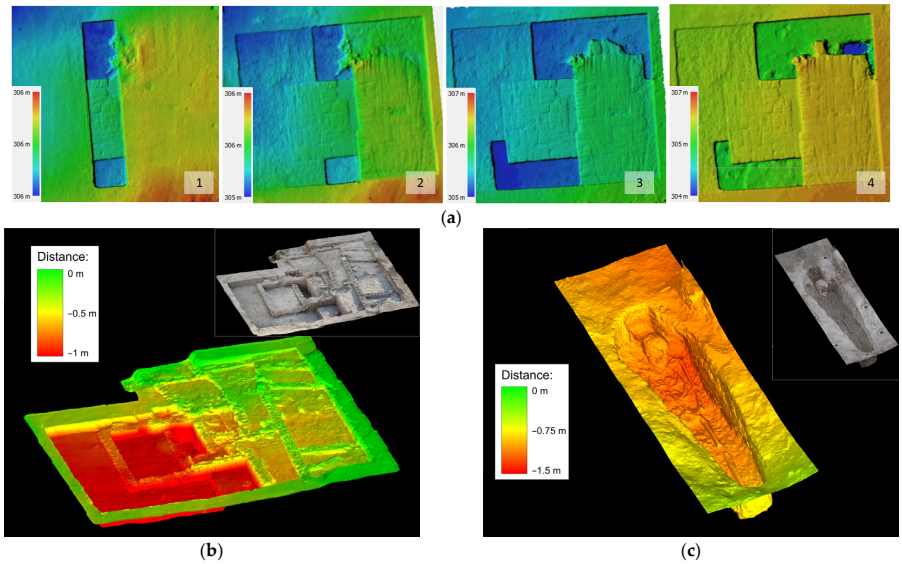

(**a**) (**b**) (**c**)

Figure 7. Examples of the modelling of archaeological work developed considering two scale levels: (**a**) representation of four DEMs of a test excavation; (**b**) distances between 3D models in test excavation; (**c**) distances between 3D models in a burial.

(**a**) (**b**) (**c**) (**d**)

Figure 8. Website developed in this study: (**a**) general view of the archaeological area; (**b**) view including an orthoimage of an excavation test (SL2–S4), including three orthoimages of burials (SL3–S3); (**c**) detailed view including the orthoimage of an excavation test as background, an orthoimage including a specific subarea, where two burials were located and two orthoimages of these burials; (**d**) 3D view of an excavation test (SL2–S4).

5. Conclusions

The methodology developed in this study integrates several geomatic techniques, in order to document an archaeological area considering several scale levels. Thus, we proposed a combination of LiDAR and photogrammetry, adapting each one to the scene to be documented. In this sense, we proposed four scale levels for these types of sites, using aerial photogrammetry and TLS for the first level related to the entire site; aerial photogrammetry and TLS for the second level related to test excavations; CRP with conventional cameras and TLS for the third level, considering elements of a few meters; and V-CRP (conventional camera mounting macro lens) and structured-light scanning at the object scale. Obviously, the inclusion of aerial LiDAR at the fist scale level could be interesting considering the dimensions of the site, although we did not apply it due to the restrictions of this type of RPAS in urban areas. On the other hand, the use of mobile mapping systems shows great potential at this scale level, due to their great efficiency of data capture.

The archaeological area analyzed in this study contained a large number of examples, in order to contrast this methodology. In this sense, the application of our approach has demonstrated its feasibility for documenting all cases with an adequate level of accuracy and resolution, considering the requirements of the project and the scale level. The presence of complex scenes such as the Roman well and burials was a major challenge, but the double data acquisition (LiDAR and photogrammetry) gave good results by combining their point clouds, in order to completely document the site. Moreover, the use of both techniques did not excessively affect the efficiency of data acquisition, as the increase of TLS acquisition time was almost compensated for by the reduction in the number of control and check points that needed to be surveyed. As examples, in the case of SL2, most of the control and check points applied to photogrammetry were obtained from the TLS point clouds and, in the case of SL3, all of them were obtained from the TLS.

This study also included a multitemporal documentation. In this sense, the methodology covered four stages, depending on the scale level. The application developed in this study allowed us to model certain scenes by acquiring data before, during, and after the excavation work. However, this aspect of our approach could be adapted to other circumstances by considering more or fewer steps in the modelling. In this sense, the documentation of all stages can be interesting, because these scenes will be removed after excavation work. The comparison of the 3D models of these stages allowed us to calculate the volume of material removed during the archaeological tests and from other areas. This can provide interesting information to compare the archaeological work developed between several dates and for estimating the volume of terrain to be removed in future works, considering the location of unexcavated areas. The multi-temporal 3D documentation provides a valuable tool for monitoring the evolution of the excavation, helping researchers to document and visualize the site at several scale levels and dates; compare geometries, dimensions, and volumes; and review contexts and material that had been previously removed during the intervention. The inclusion of multi-temporal 3D documentation may be an invaluable instrument when teaching excavation techniques and the management of a site [72].

The publication of the georeferenced products on a website provides an excellent tool for dissemination, due to the possibility of global access for all users. The visualization according to the selected zoom level and the possibility of user interaction by showing and hiding elements, navigating the map, modifying the zoom level, etc., gives this tool a great informative capacity. The system allows us to show or hide some products considering the profile of users, providing an interesting tool, not only for dissemination, but also for research and professional purposes. In addition, the visualization of 3D models represents an important aspect for the virtual documentation of the site, with a view to its future opening as an archaeological park. In this sense, we can consider this website as the first step towards a virtual archaeological park.

Future work will focus on the application of this methodology to the rest of the archaeological area, coinciding with the archaeological work of new campaigns, by incorporating

new sensors (e.g., 360-degrees cameras) and acquisition systems (e.g., portable mobile mapping systems).

Author Contributions: Conceptualization, All authors; methodology, All authors; software, J.M.G.-L.; validation, All authors; formal analysis, All authors; investigation, All authors; resources, All authors; data curation, All authors; writing—original draft preparation, A.T.M.-C.; writing—review and editing, All authors; visualization, All authors; supervision, All authors; project administration, J.L.P.-G. All authors have read and agreed to the published version of the manuscript.

Funding: This research received no external funding.

Data Availability Statement: Data were recorded at the Department of Cartographic, Geodetic and Photogrammetric Engineering, University of Jaén and can be obtained upon request. Please contact A.T.M.-C.

Conflicts of Interest: The authors declare no conflict of interest.

References

1. Lambers, K.; Remondino, F. Optical 3D measurement techniques in archaeology: Recent developments and applications. In Proceedings of the 35th International Conference on Computer Applications and Quantitative Methods in Archaeology, Berlin, Germany, 2–6 April 2007.
2. Chiabrando, F.; Di Lolli, A.; Patrucco, G.; Spanò, A.; Sammartano, G.; Teppati Losè, L. Multitemporal 3D modelling for cultural heritage emergency during seismic events: Damage assesment of S. Agostino Church in Amatrice (RI). *Int. Arch. Photogramm. Remote Sens. Spat. Inf. Sci.* **2017**, *42*, W1. [CrossRef]
3. Martínez-Fernández, A.; Benito-Calvo, A.; Campaña, I.; Ortega, A.I.; Karampaglidis, T.; de Castro, J.M.B.; Carbonell, E. 3D monitoring of Paleolithic archaeological excavations using terrestrial laser scanner systems (Sierra de Atapuerca, Railway Trench sites, Burgos, N Spain). *Digit. Appl. Archaeol. Cult. Herit.* **2020**, *19*, e00156. [CrossRef]
4. Pérez-García, J.L.; Mozas-Calvache, A.T.; Gómez-López, J.M.; Jiménez-Serrano, A. Modelling the Evolution of the Archaeological Works Developed in Qubbet El-Hawa (Aswan, Egypt). *Int. Arch. Photogramm. Remote Sens. Spat. Inf. Sci.* **2021**, *43*, 899–906. [CrossRef]
5. Ogleby, C.L.; Papadaki, H.; Robson, S.; Shortis, M.R. Comparative camera calibrations of some "off the shelf" digital cameras suited to archaeological purposes. *Int. Arch. Photogramm. Remote Sens.* **1999**, *XXXII-5/W11*, 69–75.
6. Celikoyan, T.M.; Altan, M.O.; Kemper, G.; Toz, G. Calibrating and using an Olympus camera for balloon photogrammetry. In Proceedings of the XIXth International Symposium-CIPA 2003, Antalya, Turkey, 30 September–4 October 2003.
7. Cardenal, J.; Mata, E.; Castro, P.; Delgado, J.; Hernandez, M.A.; Pérez, J.L.; Ramos, M.; Torres, M. Evaluation of a digital non metric camera (Canon D30) for the photogrammetric recording of historical buildings. *Int. Arch. Photogramm. Remote Sens. Spat. Inf. Sci.* **2004**, *XXXV-B5*, 564–569.
8. Chandler, J.H.; Fryer, J.G.; Jack, A. Metric capabilities of low-cost digital cameras for close range surface measurement. *Photogramm. Rec.* **2005**, *20*, 12–26. [CrossRef]
9. Covas, J.; Ferreira, V.; Mateus, L. 3D reconstruction with fisheye images strategies to survey complex heritage buildings. In Proceedings of the Digital Heritage 2015, Granada, Spain, 28 September–2 October 2015.
10. Fiorillo, F.; Limongiello, M.; Fernández-Palacios, B.J. Testing GoPro for 3D model reconstruction in narrow spaces. *Acta IMEKO* **2016**, *5*, 64–70. [CrossRef]
11. Barazzetti, L.; Previtali, M.; Roncoroni, F. 3D Modelling with the Samsung Gear 360. *Int. Arch. Photogramm. Remote Sens. Spat. Inf. Sci.* **2017**, *XLII-2-W3*, 85–90. [CrossRef]
12. Barazzetti, L.; Previtali, M.; Roncoroni, F. Fisheye lenses for 3D modeling: Evaluations and considerations. *Int. Arch. Photogramm. Remote Sens. Spat. Inf. Sci.* **2017**, *XLII-2/W3*, 79–84. [CrossRef]
13. Barazzetti, L.; Previtali, M.; Roncoroni, F. 3D modeling with 5K 360° videos. *Int. Arch. Photogramm. Remote Sens. Spat. Inf. Sci.* **2022**, *XLVI-2/W1-2022*, 65–71. [CrossRef]
14. Perfetti, L.; Polari, C.; Fassi, F. Fisheye Photogrammetry: Tests and Methodologies for the Survey of Narrow Spaces. *Int. Arch. Photogramm. Remote Sens. Spat. Inf. Sci.* **2017**, *XLII-2/W3*, 573–580. [CrossRef]
15. Perfetti, L.; Fassi, F. Handheld fisheye multicamera system: Surveying meandering architectonic spaces in open-loop mode—Accuracy assessment. *Int. Arch. Photogramm. Remote Sens. Spat. Inf. Sci.* **2022**, *XLVI-2/W1-2022*, 435–442. [CrossRef]
16. Colomina, I.; Molina, P. Unmanned aerial systems for photogrammetry and remote sensing: A review. *ISPRS J. Photogramm. Remote Sens.* **2014**, *92*, 79–97. [CrossRef]
17. Nex, F.; Remondino, F. UAV for 3D mapping applications: A review. *Appl. Geomat.* **2014**, *6*, 1–15. [CrossRef]
18. Campana, S. Drones in Archaeology. State-of-the-art and Future Perspectives. *Archaeol. Prospect.* **2017**, *24*, 275–296. [CrossRef]
19. Georgopoulos, A.; Karras, G.E.; Makris, G.N. The photogrammetric survey of a prehistoric site undergoing removal. *Photogramm. Rec.* **2003**, *16*, 443–456. [CrossRef]

20. Mozas-Calvache, A.T.; Pérez-García, J.L.; Cardernal-Escarcena, F.J.; Delgado, J.; Mata de Castro, E. Comparison of Low Altitude Photogrammetric Methods for Obtaining Dems and Orthoimages of Archaeological Sites. *Int. Arch. Photogramm. Remote Sens. Spat. Inf. Sci.* **2012**, *XXXIX-B5*, 577–581. [CrossRef]
21. Martínez, S.; Ortiz, J.; Gil, M.L.; Rego, M.T. Recording complex structures using close range photogrammetry: The cathedral of Santiago de Compostela. *Photogramm. Rec.* **2013**, *28*, 375–395. [CrossRef]
22. Ortiz, J.; Gil, M.L.; Martínez, S.; Rego, T.; Meijide, G. Three-dimensional Modelling of Archaeological Sites Using Close-range Automatic Correlation Photogrammetry and Low-altitude Imagery. *Archaeol. Prospect.* **2013**, *20*, 205–217. [CrossRef]
23. Blockley, P.; Morandi, S. The recording of two late Roman towers, Archaeological Museum, Milan 3D documentation and study using image-based modelling. In Proceedings of the Digital Heritage 2015, Granada, Spain, 28 September–2 October 2015.
24. Pérez-García, J.L.; Mozas-Calvache, A.T.; Gómez-López, J.M.; Jiménez-Serrano, A. Three-dimensional modelling of large archaeological sites using images obtained from masts. Application to Qubbet el-Hawa site (Aswan, Egypt). *Archaeol. Prospect.* **2018**, *26*, 121–135. [CrossRef]
25. Gómez-Lahoz, J.G.; González-Aguilera, D. Recovering traditions in the digital era: The use of blimps for modelling the archaeological cultural heritage. *J. Archaeol. Sci.* **2009**, *36*, 100–109. [CrossRef]
26. Mozas-Calvache, A.T.; Pérez-García, J.L.; Cardenal-Escarcena, F.J.; Mata-Castro, E.; Delgado-García, J. Method for photogrammetric surveying of archaeological sites with light aerial platforms. *J. Archaeol. Sci.* **2012**, *39*, 521–530. [CrossRef]
27. Brutto, M.L.; Meli, P. Computer vision tools for 3D modelling in archaeology. *Int. J. Herit. Digit. Era* **2012**, *1*, 1–6. [CrossRef]
28. McCarthy, J. Multi-image photogrammetry as a practical tool for cultural heritage survey and community engagement. *J. Archaeol. Sci.* **2014**, *43*, 175–185. [CrossRef]
29. Ullman, S. The interpretation of structure from motion. *Proc. R. Soc. B* **1979**, *203*, 405–426.
30. Koenderink, J.J.; Van Doorn, A.J. Affine structure from motion. *J. Opt. Soc. Am. A* **1991**, *8*, 377–385. [CrossRef]
31. Lowe, D.G. Distinctive image features from scale-invariant keypoints. *Int. J. Comput. Vis.* **2004**, *60*, 91–110. [CrossRef]
32. Szeliski, R. *Computer Vision: Algorithms and Applications*; Springer: London, UK, 2011.
33. Scharstein, D.; Szeliski, R. A taxonomy and evaluation of dense two-frame stereo correspondence algorithms. *Int. J. Comput. Vis.* **2002**, *47*, 7–42. [CrossRef]
34. Seitz, S.M.; Curless, B.; Diebel, J.; Scharstein, D.; Szeliski, R. A comparison and evaluation of multi-view stereo reconstruction algorithms. In Proceedings of the IEEE Computer Society Conference on Computer Vision and Pattern Recognition, New York, NY, USA, 17–22 June 2006.
35. Furukawa, Y.; Hernández, C. Multi-view stereo: A tutorial. *Found. Trends Comput. Graph. Vis.* **2015**, *9*, 1–148. [CrossRef]
36. Westoby, M.J.; Brasington, J.; Glasser, N.F.; Hambrey, M.J.; Reynolds, J.M. 'Structure-from-Motion' photogrammetry: A low-cost, effective tool for geoscience applications. *Geomorphology* **2012**, *179*, 300–314. [CrossRef]
37. Risbøl, O.; Gustavsen, L. LiDAR from drones employed for mapping archaeology–Potential, benefits and challenges. *Archaeol. Prospect.* **2018**, *25*, 329–338. [CrossRef]
38. Casana, J.; Laugier, E.J.; Hill, A.C.; Reese, K.M.; Ferwerda, C.; McCoy, M.D.; Ladefoged, T. Exploring archaeological landscapes using drone-acquired LiDAR: Case studies from Hawai'i, Colorado, and New Hampshire, USA. *J. Archaeol. Sci. Rep.* **2021**, *39*, 103133. [CrossRef]
39. Coluzzi, R.; Lanorte, A.; Lasaponara, R. On the LiDAR contribution for landscape archaeology and palaeoenvironmental studies: The case study of Bosco dell'Incoronata (Southern Italy). *Adv. Geosci.* **2010**, *24*, 125–132. [CrossRef]
40. Canuto, M.A.; Estrada-Belli, F.; Garrison, T.G.; Houston, S.D.; Acuña, M.J.; Kováč, M.; Marken, D.; Nondédéo, P.; Auld-Thomas, L.; Castanet, C.; et al. Ancient lowland Maya complexity as revealed by airborne laser scanning of northern Guatemala. *Science* **2018**, *361*, eaau0137. [CrossRef]
41. Ahmon, J. The application of short-range 3D laser scanning for archaeological replica production: The Egyptian tomb of Seti I. *Photogramm. Rec.* **2004**, *19*, 111–127. [CrossRef]
42. Fernández-Palacios, B.J.; Rizzi, A.; Remondino, F. Etruscans in 3D-Surveying and 3D modeling for a better access and understanding of heritage. *Virtual Archaeol. Rev.* **2013**, *4*, 85–89. [CrossRef]
43. Nabil, M.; Betrò, M.; Metwallya, M.N. 3D reconstruction of ancient Egyptian rockcut tombs: The case of Midan 05. *Int. Arch. Photogramm. Remote Sens. Spat. Inf. Sci.* **2013**, *XL-5/W2*, 443–447. [CrossRef]
44. De Lima, R.; Vergauwen, M. From TLS recoding to VR environment for documentation of the Governor's Tombs in Dayr al-Barsha, Egypt. In Proceedings of the 2018 IEEE International Symposium on Mixed and Augmented Reality Adjunct (ISMAR-Adjunct), Munich, Germany, 16–20 October 2018.
45. Echeverría, E.; Celis, F.; Morales, A.; da Casa, F. The Tomb of Ipi: 3D Documentation in a Middle Kingdom Theban Necropolis (Egypt, 2000 BCE). *Int. Arch. Photogramm. Remote Sens. Spat. Inf. Sci.* **2019**, *XLII-2/W9*, 319–324. [CrossRef]
46. Colonnese, F.; Carpiceci, M.; Inglese, C. Conveying Cappadocia. A new representation model for rock-cave architecture by contour lines and chromatic codes. *Virtual Archaeol. Rev.* **2016**, *7*, 13–19. [CrossRef]
47. Pérez-García, J.L.; Mozas-Calvache, A.T.; Barba-Colmenero, V.; Jiménez-Serrano, A. Photogrammetric studies of inaccessible sites in archaeology: Case study of burial chambers in Qubbet el-Hawa (Aswan, Egypt). *J. Archaeol. Sci.* **2019**, *102*, 1–10.
48. Mozas-Calvache, A.T.; Pérez-García, J.L.; Gómez-López, J.M.; de Dios, J.M.; Jiménez-Serrano, A. 3D models of the QH31, QH32 and QH33 tombs in Qubbet el Hawa (Aswan, Egypt). *Int. Arch. Photogramm. Remote Sens. Spat. Inf. Sci.* **2020**, *XLIII-B2-2020*, 1427–1434. [CrossRef]

49. Zlot, R.; Bosse, M. Three-dimensional mobile mapping of caves. *J. Cave Karst Stud.* **2014**, *76*, 191–206. [CrossRef]
50. Farella, E.M. 3D mapping of underground environments with a hand-held laser scanner. *Boll. Soc. Ital. Fotogramm. Topogr.* **2016**, *2*, 1–10.
51. Di Stefano, F.; Torresani, A.; Farella, E.M.; Pierdicca, R.; Menna, F.; Remondino, F. 3D surveying of underground built heritage: Opportunities and challenges of mobile technologies. *Sustainability* **2021**, *13*, 13289. [CrossRef]
52. Kadobayashi, R.; Kochi, N.; Otani, H.; Furukawa, R. Comparison and evaluation of laser scanning and photogrammetry and their combined use for digital recording of cultural heritage. *Int. Arch. Photogramm. Remote Sens. Spat. Inf. Sci.* **2004**, *35*, 401–406.
53. Alshawabkeh, Y.; Haala, N. Integration of digital photogrammetry and laser scanning for heritage documentation. *Int. Arch. Photogramm. Remote Sens.* **2004**, *35*, 1–6.
54. Guarnieri, A.; Remondino, F.; Vettore, A. Digital photogrammetry and TLS data fusion applied to Cultural Heritage 3D modeling. *Int. Arch. Photogramm. Remote Sens. Spat. Inf. Sci.* **2006**, *36 Pt 5*, 1–6.
55. Grussenmeyer, P.; Landes, T.; Voegtle, T.; Ringle, K. Comparison methods of terrestrial laser scanning, photogrammetry and tacheometry data for recording of cultural heritage buildings. *Int. Arch. Photogramm. Remote Sens. Spat. Inf. Sci.* **2008**, *XXXVII/B5*, 213–218.
56. Gajski, D.; Solter, A.; Gašparović, M. Applications of macro photogrammetry in archaeology. *Int. Arch. Photogramm. Remote Sens. Spat. Inf. Sci.* **2016**, *XLI-B5*, 263–266. [CrossRef]
57. Marziali, S.; Dionisio, G. Photogrammetry and macro photography. The experience of the MUSINT II Project in the 3D digitizing process of small size archaeological artifacts. *Stud. Digit. Herit.* **2017**, *1*, 298–309. [CrossRef]
58. Boehler, W.; Heinz, G.; Marbs, A. The potential of non-contact close range laser scanners for cultural heritage recording. *Int. Arch. Photogramm. Remote Sens. Spat. Inf. Sci.* **2002**, *34*, 430–436.
59. Farjas, M.; García-Lázaro, F.J.; Jiménez, D.; Bondier, J.J.; Jimeno, J.Z.; Moreno, J.M. Geodesic Approach to an Artefact-3D Scanner Virtual Modeling versus Archaeological Tracings (First Part). In Proceedings of the 15th International Conference on Virtual Systems and Multimedia, Vienna, Austria, 9–12 September 2009.
60. McPherron, S.P.; Gernat, T.; Hublin, J.J. Structured light scanning for high-resolution documentation of in situ archaeological finds. *J. Archaeol. Sci.* **2009**, *36*, 19–24. [CrossRef]
61. Scafuri, M.P.; Rennison, B. Scanning the HL Hunley: Employing a structured-light scanning system in the archaeological documentation of a unique maritime artifact. *J. Archaeol. Sci. Rep.* **2016**, *6*, 302–309.
62. Maté-González, M.Á.; Aramendi, J.; González-Aguilera, D.; Yravedra, J. Statistical comparison between low-cost methods for 3D characterization of cut-marks on bones. *Remote Sens.* **2017**, *9*, 873. [CrossRef]
63. The American Society for Photogrammetry and Remote Sensing (ASPRS). ASPRS Positional Accuracy Standards for Digital Geospatial Data. *Photogramm. Eng. Remote Sens.* **2015**, *81*, A1–A26. [CrossRef]
64. Gómez-López, J.M.; Pérez-García, J.L.; Mozas-Calvache, A.T.; Delgado-García, J. Mission Flight Planning of RPAS for Photogrammetric Studies in Complex Scenes. *ISPRS Int. J. Geo-Inf.* **2020**, *9*, 392. [CrossRef]
65. Waldhäusl, P.; Ogleby, C.L. 3 × 3 rules for simple photogrammetric documentation of architecture. *Int. Arch. Photogramm. Remote Sens.* **1994**, *30*, 426–429.
66. CIPA Heritage Documentation. The Photogrammetric Capture. The '3×3' Rules. Available online: https://www.cipaheritagedocumentation.org/ (accessed on 16 February 2023).
67. ArcGIS API Developers. Zoom Levels and Scale. Available online: https://developers.arcgis.com/documentation/mapping-apis-and-services/reference/zoom-levels-and-scale/ (accessed on 16 February 2023).
68. Open Street Map. Zoom levels. Available online: https://wiki.openstreetmap.org/wiki/Zoom_levels (accessed on 16 February 2023).
69. Leaflet JavaScript Library. Available online: https://leafletjs.com/ (accessed on 16 February 2023).
70. Potenziani, M.; Callieri, M.; Dellepiane, M.; Corsini, M.; Ponchio, F.; Scopigno, R. 3DHOP: 3D heritage online presenter. *Comput. Graph.* **2015**, *52*, 129–141. [CrossRef]
71. 3D Heritage Online Presenter (3DHOP). Available online: https://www.3dhop.net/ (accessed on 16 February 2023).
72. Dellepiane, M.; Dell'Unto, N.; Callieri, M.; Lindgren, S.; Scopigno, R. Archeological excavation monitoring using dense stereo matching techniques. *J. Cult. Herit.* **2013**, *14*, 201–210. [CrossRef]